

Research Article

A Neural Network Predictive Model for Welded Marine Pipeline Internal Corrosion

¹Abdulwahab A. Alnaqi, ²N.S. Reddy, ¹Khaled Alawadhi, ¹Ahmad E. Murad and ¹Hasan A. Mulla Ali

¹Department of Automotive and Marine Engineering Technology, College of Technological Studies-
PAAET, Kuwait

²School of Material Science and Engineering, Gyeongsang National University, Jinju, 660-701,
Republic of Korea

Abstract: In spite of the huge success of computational chemistry in corrosion studies, most of the ongoing research on the inhibition of preferential weld corrosion is restricted to laboratory work. In the present study, a nondeterministic artificial intelligence model is proposed, the aim being to more accurately predict the occurrence of corrosion in the Heat Affected Zone (HAZ), which is most exposed to corrosion risk. The prediction of corrosion rates has become an important challenge for the engineering community. For industry, one of the more important aspects of corrosion is the HAZ for welded carbon steel in CO₂ environments. Nowadays, data from various sources (e.g., temperature and velocity), for both inhibited and non-inhibited CO₂ solutions, can be fed into neural networks, allowing them to be used for data processing. An artificial neural network is proposed for the prediction of corrosion in the HAZ. A phenomenal outcome for the prediction of corrosion in the HAZ was proposed with the learning ability of an artificial neural network using software, through which training of 406 sets of data using the Leven Berg-Marquardt algorithm were obtained from experimental data. The training sets were developed for three levels of corrosion (mild, moderate and severe) through the Artificial Neural Network (ANN) and resulted in a trend which took the form of an incremental parabolic curve. This study presents an artificial neural network model which simulates the complex and nonlinear atmospheric corrosion process observed in experimental data. The correlation statistics (R) in the ANN proved to be 90% accurate. The test results were validated to confirm the efficacy of the developed ANN model for prediction of corrosion rate and good performance was observed. The interactions between the inputs were estimated by performing a sensitivity analysis based on the developed model. Since the model results from this research showed good agreement with experimentally obtained corrosion rates, it could now be widely applied in corrosion studies.

Keywords: Artificial Neural Networks (ANN), corrosion, prediction

INTRODUCTION

Corrosion presents a challenge for design and corrosion engineers in the oil and gas production and transportation industries. Marine oil field corrosion manifests itself in several forms, which include the "sweet corrosion" caused by carbon dioxide (CO₂) gas in various marine pipeline operations. The major parameters influencing the rate are temperature, pressure, flow and salinity (Turgoose and Palmer, 2005).

Carbon steel welded marine pipelines are used extensively in the oil and gas industry for sub-sea applications. The cost of marine pipeline corrosion is a considerable part of the investment in subsea projects for long-distance and large-diameter pipelines. Better

understanding and control of the corrosion of carbon steel could increase its applicability and, therefore, have a sizeable economic impact (Nyborg, 2005). Prediction of the rate of corrosion of steel structures in global marine environments is a challenging task due to the wide variation in the parameters involved.

A recent survey found that around 36% of failures in offshore pipelines were attributable to (localized) corrosion in welds. It is known that the most severe form is pitting corrosion and that this is worse for the Heat Affected Zone (HAZ) than for either the weld zone or the parent metal. This is due to the nature of its formation during the welding process, with a significant short-term thermal gradient occurring between the weld metal and the parent metal followed by quite rapid cooling (Chaves and Melchers, 2014).

Corresponding Author: Abdulwahab A. Alnaqi, Department of Automotive and Marine Engineering Technology, College of Technological Studies-PAAET, Kuwait

This work is licensed under a Creative Commons Attribution 4.0 International License (URL: <http://creativecommons.org/licenses/by/4.0/>).

Raja Dhas and Somasundaram (2013) were able to make predictions about the heat affected zone associated with a SAW process, which was a useful aid to determining the quality of a weld and avoiding the residual stress and distortion that can lead to the failure of the weldment.

Although experimental studies are straightforward, they are often expensive and time-consuming. Alternatively, modeling is useful and a powerful tool in improving our understanding of the corrosion process. It also helps construction and corrosion engineers by predicting the life of a marine pipeline in a given environment. Several models for predicting CO₂ corrosion are to be found in the literature (Malinov *et al.*, 2000; Metzbowyer *et al.*, 2001). These models are mainly based on laboratory data and in some cases are validated by field data. They can be classified as mechanistic models, semi-empirical models or empirical models (De Masi *et al.*, 2014).

In the past few years, there has been a growing interest in ANN modeling of various aspects of the marine environment. ANN models have been developed to predict different correlations and phenomena in steels, aluminum alloys and titanium alloys (Paul, 2012). However, not many neural networks have been applied to the analysis of non-homogeneous material conditions, such as those involved with corrosion rates in welded pipelines. This is because prediction modeling is complicated due to metallurgical variation of the welded region, including the Weld Metal (WM), Heat Affected Zone (HAZ) and Parent Material (PM).

Neural networks can learn both static and dynamic properties autonomously, based on historical measurements and then act in such a way that a better solution is obtained under unknown environmental conditions (Alawadhi and Robinson, 2011). In the present study, a nondeterministic artificial intelligence model is proposed, the aim being to more accurately predict the occurrence of corrosion in the HAZ section, which is most exposed to corrosion risk.

Experimental procedure: A series of experiments was performed in-house to identify the current density (I_{corr}) of the HAZ of welded marine pipelines. A cylindrical working, HAZ representative electrode, made of API X56 steel, was used in the experiments. The experiment was performed in a glass cell and used a Saturated Calomel Electrode as the reference electrode. The counter electrode was a platinum wire. All the tests were carried out at three different temperatures, 25, 50 and 70°C, under 1 bar pressure. Cell temperature was controlled by a hot plate with thermocouple feedback. In order to remove oxygen from the test solution, CO₂ gas was bubbled into the test solution for a period of 30 min prior to the test. The I_{corr} was obtained under static and dynamic (turbulent flow) conditions using a rotating cylinder electrode, with an inhibitor and

without an inhibitor. In dynamic conditions, a rotational speed range of 1000 rpm to 5000 rpm was used. Polarization experiments were carried out as per ASTM standard methods (Scully, 2000; Oluwole and Idusuyi, 2012; ASTM G59-97, 2003; ASTM G5-94, 2004), using an ACM potential stat to impose various potentials on the cylinder electrode while simultaneously measuring the current. The potential was then scanned 10 mV above and below this value, at a scan rate of 10 mV min. The I_{corr} of the HAZ region was measured by uncoupling the electrode of the RCE in turn and carrying out Linear Polarization Resistance measurements (LPR).

MODELING METHODOLOGY

The objective of the study was to predict HAZ corrosion rates using ANN modeling. The data used for model development in the training and testing stages were collected from literature (Alawadhi and Robinson, 2011). ANN models create a correlation between input and target output with the help of hidden neurons in hidden layers. A total of 42 data sets were available from experiments and these were randomly divided into 30 training and 12 testing sets. The seven input parameters considered in the present work were temperature, inhibitor, speed, flow velocity, Reynolds number, mass shear stress and Sherwood number and the output was corrosion rate. The data sets and their descriptive statistics are listed in Table 1 and 2, respectively. Feed forward neural networks with backpropagation algorithms were used to develop the model. A root mean squared error of 0.000036 and mean average error of 0.028848 after 15000 iterations was achieved. The architecture consisted of 2 hidden layers, each layer consisting of 6 hidden neurons (7-6-6-1), a learning rate of 0.3 and momentum term of 0.6.

RESULTS AND DISCUSSION

LPR test: The variation in the experimental and numerical I_{corr} values for the 3.5% NaCl solution, with and without the addition of the inhibitors at different temperatures, is given in Fig. 1 and 2, respectively. It is known that, once polarization resistance is determined, calculation of I_{corr} requires knowledge of Tafel constants and these constants can be determined from experimental polarization curves. However, when the results show polarization resistance values within the same order of magnitude, it is necessary to use more accurate values derived from the Tafel slopes in order to perform a consistent analysis of the results (ASTM G59-97, 2003 and ASTM G5-94, 2004). Therefore, I_{corr} values were obtained from polarization resistance measurements using the Stern-Geary expression (Stansbury and Buchanan, 2000). The input parameters were: Density = 7.8 g/cm³; Tafel constants, $b_a = b_c = 60$ mV/Decade; Equivalent weight, 28 grams; Scan rate

Table 1: Experimental and ANN simulated HAZ corrosion rate results' (*:0 indicates uninhibited solution; 1 indicates inhibited solution (30 ppm inhibitor))

No.	Temp	Inhibitor code	Speed	Flow velocity	Reynolds number	Mass shear stress	Sherwood number	CR	Train/test
1	20	0	0	0	0	0	0	0.644017	Train
2	20	0	500	0.52	9950	1.40	464	0.802894	Train
3	20	0	1000	1.05	20000	4.55	753	0.858647	Train
4	20	0	2000	2.09	40100	14.8	1220	0.996315	Test
5	20	0	3000	3.14	60100	29.5	1620	1.216025	Train
6	20	0	4000	4.19	80200	48.0	1980	1.425702	Test
7	20	0	5000	5.24	100000	70.2	2330	1.579880	Train
8	50	0	0	0	0	0.00	0	1.745996	Train
9	50	0	500	0.52	9950	1.40	464	1.932178	Test
10	50	0	1000	1.05	20000	4.55	753	2.140585	train
11	50	0	2000	2.09	40100	14.8	1220	2.122805	train
12	50	0	3000	3.14	60100	29.5	1620	2.353564	test
13	50	0	4000	4.19	80200	48.0	1980	2.306066	train
14	50	0	5000	5.24	100000	70.2	2330	2.339975	train
15	70	0	0	0	0	0.00	0	1.019048	test
16	70	0	500	0.52	9950	1.40	464	1.131951	train
17	70	0	1000	1.05	20000	4.55	753	1.114044	test
18	70	0	2000	2.09	40100	14.8	1220	1.009777	train
19	70	0	3000	3.14	60100	29.5	1620	0.910336	train
20	70	0	4000	4.19	80200	48.0	1980	1.157859	test
21	70	0	5000	5.24	100000	70.2	2330	1.712214	Train
22	20	1	0	0	0	0.00	0	0.006731	train
23	20	1	500	0.52	9950	1.40	464	0.008255	Train
24	20	1	1000	1.05	20000	4.55	753	0.011938	test
25	20	1	2000	2.09	40100	14.8	1220	0.012954	Train
26	20	1	3000	3.14	60100	29.5	1620	0.012065	Train
27	20	1	4000	4.19	80200	48.0	1980	0.017272	Train
28	20	1	5000	5.24	100000	70.2	2330	0.042672	test
29	50	1	0	0	0	0.00	0	0.034925	test
30	50	1	500	0.52	9950	1.40	464	0.093599	Train
31	50	1	1000	1.05	20000	4.55	753	0.116332	Train
32	50	1	2000	2.09	40100	14.8	1220	0.126492	test
33	50	1	3000	3.14	60100	29.5	1620	0.130302	Train
34	50	1	4000	4.19	80200	48.0	1980	0.199771	Train
35	50	1	5000	5.24	100000	70.2	2330	0.189484	Train
36	70	1	0	0	0	0.00	0	0.112141	Train
37	70	1	500	0.52	9950	1.40	464	0.083693	test
38	70	1	1000	1.05	20000	4.55	753	0.060198	Train
39	70	1	2000	2.09	40100	14.8	1220	0.062357	Train
40	70	1	3000	3.14	60100	29.5	1620	0.194691	test
41	70	1	4000	4.19	80200	48	1980	0.158877	Train
42	70	1	5000	5.24	100000	70.2	2330	0.138938	Train

Table 2: Descriptive statistics of the data used for modeling

Input/output	Minimum	Maximum	Mean	SD
Temperature	20	70	46.6700	35.36000
Inhibitor	0	1	0.50000	0.710000
Speed	0	5000	2214.28	3535.530
Flow velocity	0	5.24	2.32000	3.710000
Reynolds number	0	100000	44335.7	70710.68
Mass shear stress	0	70.2	24.0600	49.64000
Sherwood number	0	2330	1195.30	1647.560
Corrosion rate	0.006731	2.353564	0.76980	0.360000

= 166 μV/s, which corresponds to 10 mV/min; Potential Shift, -10 mV, +10 mV and B = 13 mV:

$$I_{corr} = \frac{babc}{2.3 Rp(Ba + Bc)} = \frac{B}{Rp}$$

It was clear that the simulated results are consistent with those from the experiments. Increasing temperature and rotational speed led to an increase in current density, from 99.22 mA/cm² to 147.24 mA/cm² at 25°C, from 166.5 mA/cm² to 201.891 mA/cm² at 50°C and from 166.5 mA/cm² to 201.896 mA/cm² at 70°C, all in the absence of inhibitors. Under

static conditions, visual examination found that a dark grey film was formed on the metal surface. However, when the rotational speed increased, it was observed that, at all temperatures, current density increased linearly. This was attributed to the fact that the dark grey surface film that forms under static conditions, which appears to be partially protective, can be partly removed when under high shear stress. As a result, the film had an open porous structure which explains why it offered little corrosion protection (Pardo *et al.*, 2010). Another observation was that, at 70°C, there was more protection for the HAZ than at other temperatures for the same rotational speed, indicating that when these

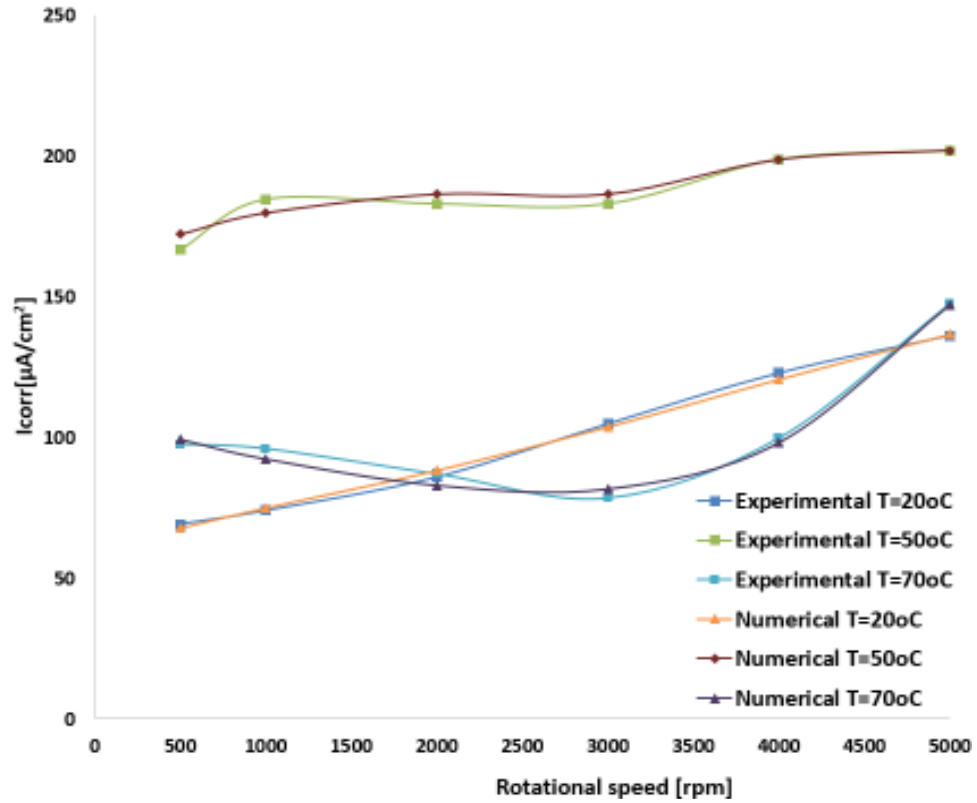


Fig. 1: Effect of temperature and rotational speed on I_{corr} values under uninhibited conditions

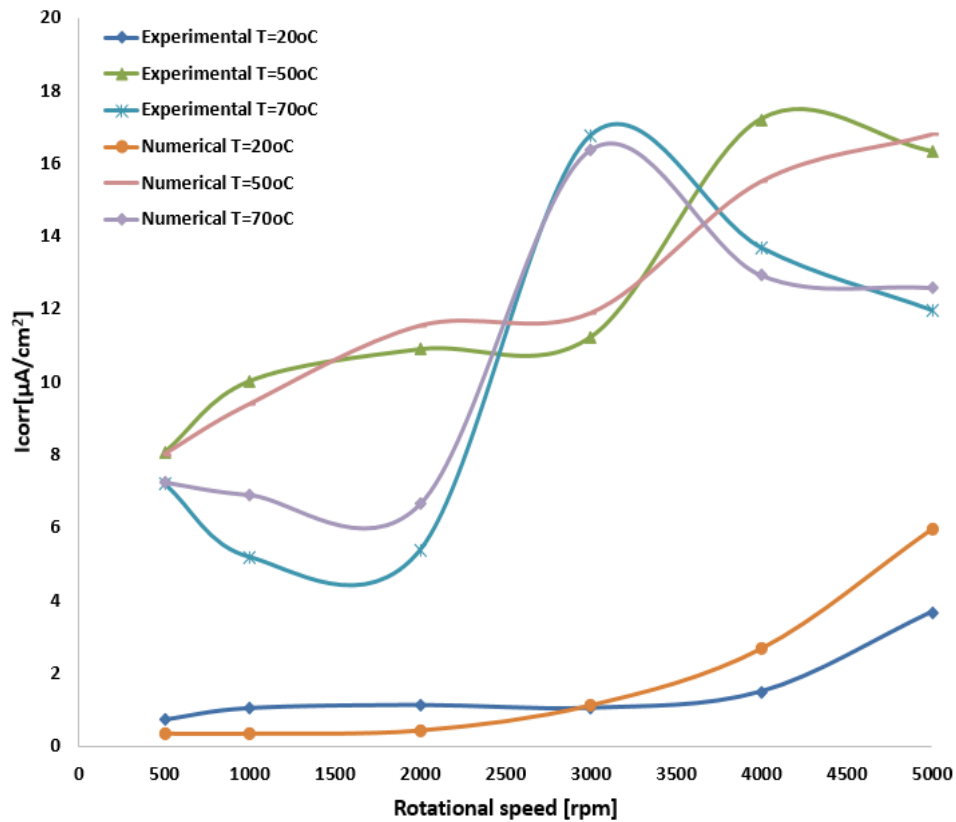


Fig. 2: Effect of temperature and rotational speed on I_{corr} values under inhibited conditions

kinds of film are formed, their stability and protectiveness increase with temperature, especially for temperatures above 60°C (Alawadhi and Robinson, 2011).

The current density was measured at various temperatures and at different rotational speeds in the presence of the corrosion inhibitor. However, current densities were considerably lower than those under uninhibited conditions. Under flowing conditions, inhibitors seem to become better attached to the HAZ, providing good corrosion protection, especially at room temperature. However, for the HAZ at 50 and 70°C, especially at 5000 rpm, an increase in current density was noticed and this was thought to be due to the partial removal of the inhibitor film formed on the metal surface. It was found that the inhibitor remained on the metal surface for a few hours, but as the rotation speed increased, it became detached from the surface leaving active sites, increasing susceptibility toward localized types of corrosion. There was a marginal difference in the current density curves at the different rotation speeds. As soon as the rotation speed increased, the I_{corr} value increased slightly obtaining the highest value at 3000 rpm, but it decreased again with a further increase

in the rotation speed to 5000 rpm, as seen for the uninhibited solution.

At room temperature, the lines are nearly horizontal, indicating that rotational speed had very little effect. In general, the I_{corr} under inhibited conditions was two or three times lower than under uninhibited conditions. As previously stated, inhibitors perform differently under flow conditions, as the flow can increase mass transport of inhibitor molecules leading to their concentration at the metal surface. This effect can improve inhibitor performance (Nafday and Nestic, 2005).

ANN modeling results: The model predictions for the training and test data are shown in Fig. 3. The Pearson r values and adjusted R squared values, which indicate the model's predictive efficiency, were calculated and are shown in Fig. 3. For training data, these values are near to one. Even for unseen test data, the values are in good agreement with experimental values and the average error in the prediction for 12 samples is 0.055. Thus, the ANN model will be helpful in the accurate prediction of corrosion rates and useful to industry.

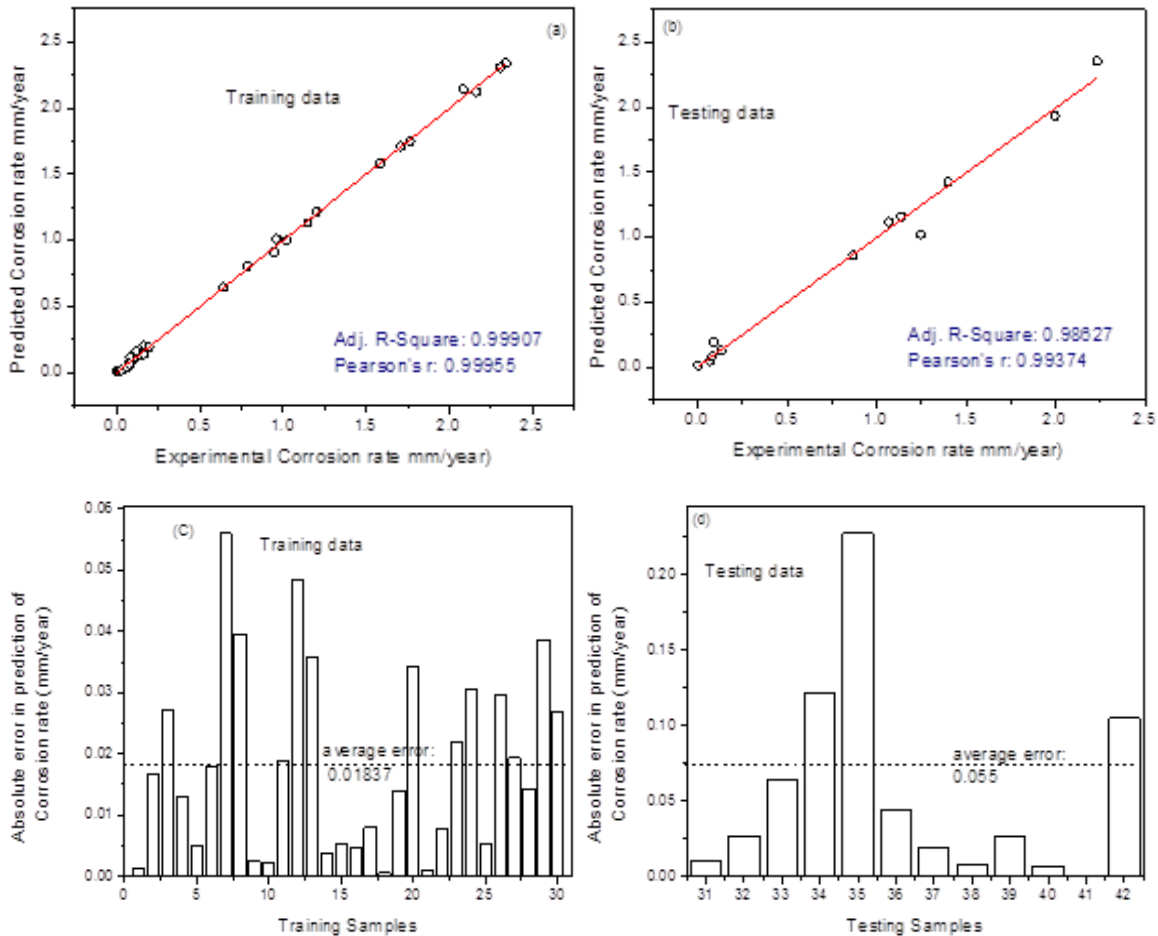


Fig. 3: Predicted and experimental corrosion rates for the HAZ; (a): training data; (b): testing data and the absolute errors of; (c): training data and (d): testing data

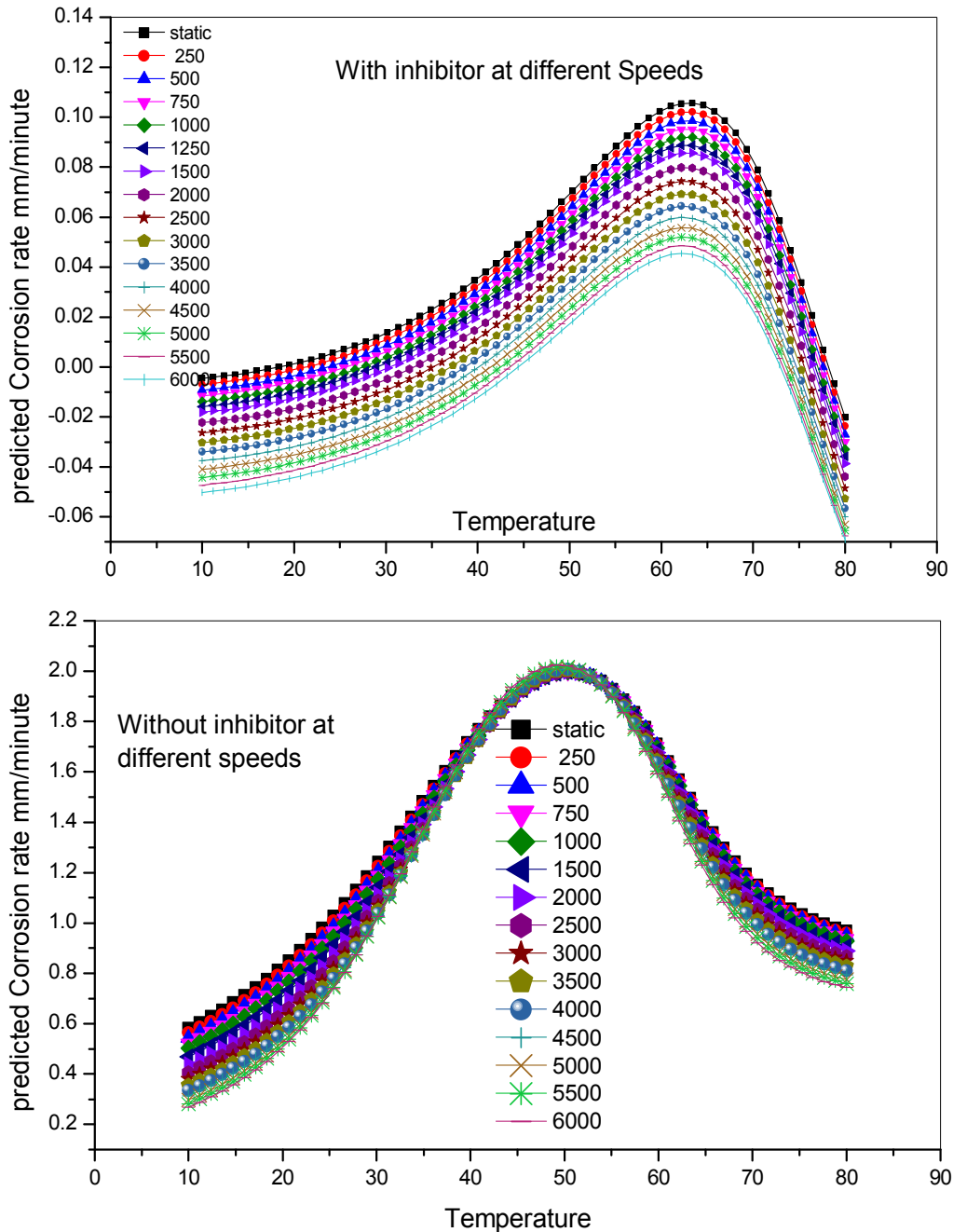


Fig. 4: Predicted corrosion rate versus temperature for various speeds of rotation

A sensitivity analysis was carried out on the trained model testing the predictions by varying temperature with and without an inhibitor at different speeds. In the presence of an inhibitor, with increasing speed and temperature, the corrosion rate increases up to 65°C. Without an inhibitor, the highest corrosion rate was observed at around 50°C, at all speeds. The predictions without an inhibitor showed higher corrosion rates than with an inhibitor at all temperatures and speeds. This is in good agreement with practical observation. The corrosion experiments on the steels were conducted at

20, 50 and 70°C and at 500, 1000, 2000, 3000, 4000 and 5000 rpm speeds.

The model can also predict at intermediate values of temperature (30, 35, 45, etc.) and at various speed values (1250, 1500, 2500, etc.), which will be useful for analyzing optimum conditions for lower corrosion values

The training network result showed that all data were successfully modeled. One distinguishing characteristic of an ANN is its adaptability which requires a unique information flow design, as shown in Fig. 4.

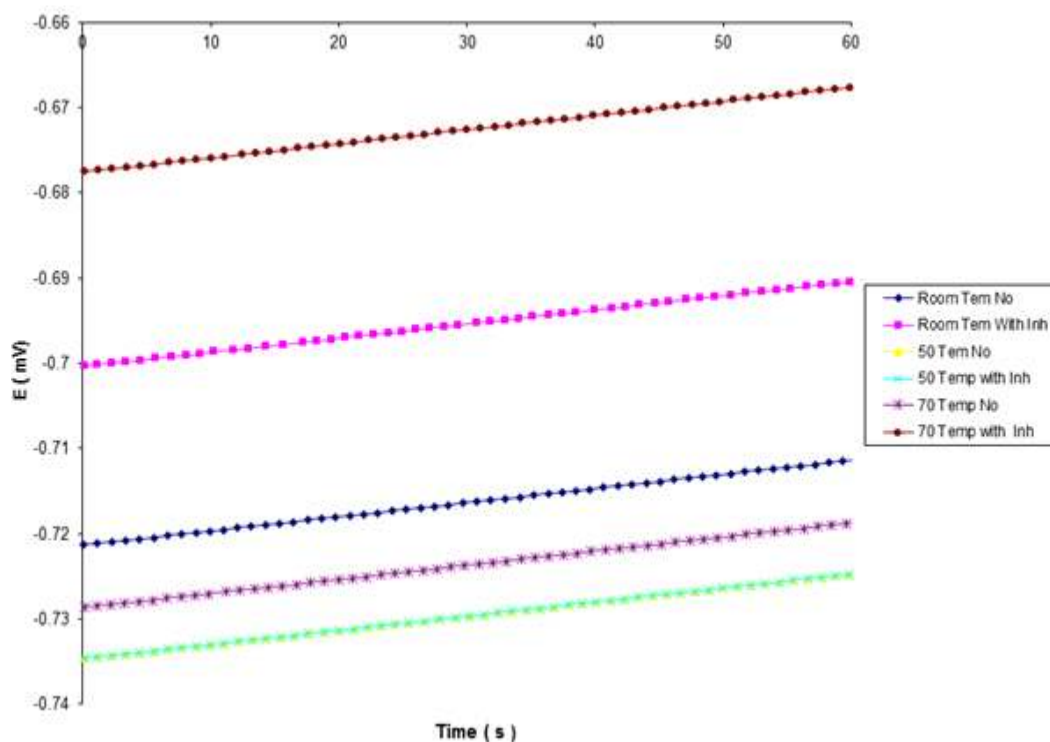


Fig. 5: Potential variations at different rotation speeds and different temperatures under inhibited and uninhibited conditions

Corrosion potential measurements: It is known that a simple way to study the film formation of materials in a solution is to monitor the E_{corr} as a function of time, as shown in Fig. 5. A rise in potential in the positive direction indicates the formation of a passive film, a steady potential indicates that the film remains intact and protective and a drop in potential in the negative direction indicates breaks in the film, dissolution of the film, or no film formation (Nafday and Nescic, 2005). Temperature and rotation speed are factors that affect the electrochemical behavior of a metal in a corrosive environment. The metal inhibitor interactions can also be influenced by this factor. Figure 5 shows the variation of the measured E_{corr} with time exposure in the test solution in both conditions (brine with and without inhibitor). Corrosion potential significantly changes as a function of temperature and the corrosion potential evolution as a function of time is the best qualitative method for monitoring interface modification between a metal and its environment (Alawadhi and Robinson, 2011). The OCP (Open Circuit Potential) of mild steel was monitored over 60 minutes, from the moment of immersion in the test solution, at three different temperatures (room, 50 and 70°C). The influence of the rotation speed of 5000 rpm on the open circuit potential of the HAZ at room temperature stabilized between -0.7 mV and -0.69 mV under uninhibited conditions, but when the inhibitor was added, the sample showed the effect of the forming inhibitor layer, increasing the OCP linearly in the

positive direction. In addition, it is important to note that at 50°C, either with or without the inhibitor, the corrosion potential values slightly increase with time. E_{corr} values with the inhibitor are slightly higher than those observed without the inhibitor. This behavior shows that the E_{corr} of the HAZ zone of the welded carbon steel has been slightly affected by the inhibitor in the test environment. At 70°C, it was found that the OCP becomes more positive in inhibited solution than in uninhibited solution. This means that the surface becomes nobler in the presence of the inhibitor. Moreover, it becomes nobler with increased temperature due to the presence of more inhibitor on the metal surface, leading to the formation of an inhibitor film and increasingly positive values of OCP. According to some researchers, under uninhibited conditions, with a temperature below (60°C), the solubility of FeCO_3 is high; hence the protective films may still build up but are not protective.

CONCLUSION

A neural network has been developed for the prediction of HAZ corrosion in X65 carbon steel pipelines. Various aggressive temperatures and rotational speeds are taken into consideration, for both inhibited and uninhibited conditions. The data obtained showed a good agreement between the experimental data and simulation results, confirming that it is an effective approach for corrosion prediction.

Under uninhibited conditions, it was clear that both increasing temperature and rotational speed led to an increase in current density. In addition, current densities were considerably lower and this could be attributed to the effect of the inhibitor which seems to become better attached to the HAZ, providing good corrosion protection, especially at room temperature.

Under aggressive conditions, high temperature and a high rotational speed of 5000 rpm, an increasing current density was noticed and this was thought to be due to the partial removal of the inhibitor film formed on the HAZ.

REFERENCES

- Alawadhi, K. and M. Robinson, 2011. Preferential weld corrosion of X65 pipeline steel in flowing brines containing carbon dioxide. *Corros. Eng. Sci. Technol.*, 46(4): 318-329.
- ASTM G5-94, 2004. Standard Reference Test Method for Making Potentiostatic and Potentiodynamic Anodic Polarization Measurements. Retrieved from: <http://www.astm.org/DATABASE.CART/HISTORICAL/G5-94R04.htm>.
- ASTM G59-97, 2003. Standard Test Method for Conducting Potentiodynamic Polarization Resistance Measurements. Retrieved from: <http://www.astm.org/DATABASE.CART/HISTORICAL/G59-97R03.htm>.
- Chaves, I.A. and R.E. Melchers, 2014. External corrosion of carbon steel pipeline weld zones. *Int. J. Offshore Polar*, 24(1): 68-74.
- De Masi, G., R. Vichi, M. Gentile, R. Bruschi and G. Gabetta, 2014. A neural network predictive model of pipeline internal corrosion profile. *Proceeding of the 1st International Conference on Systems Informatics, Modelling and Simulation (SIMS '14)*, pp: 20-25.
- Malinov, S., W. Sha and Z. Guo, 2000. Artificial neural network modelling of crystallization temperatures of the Ni-P based amorphous alloys material. *Mater. Sci. Eng. A*, 283: 1-218.
- Metzbower, E.A., J.J. DeLoach, S.H. Lalam and H.K.D.H. Bhadeshia, 2001. Neural network analysis of strength and ductility of welding alloys for high strength low alloy shipbuilding steels. *Sci. Technol. Weld. Joi.*, 6(2): 116-124.
- Nafday, O.A. and S. Nestic, 2005. Iron carbonate scale formation and CO₂ corrosion in the presence of acetic acid. *NACE CORROSION*, 2005, Paper No. 05295, NACE International.
- Nyborg, R., 2005. Controlling internal corrosion in oil and gas pipelines. *Bus. Brief. Explorat. Prod. Oil Gas Rev.*, 2: 70-74.
- Oluwole, O. and N. Idusuyi, 2012. Artificial neural network modeling for al-zn-sn sacrificial anode protection of low carbon steel in saline media. *Am. J. Mater. Sci.*, 2(3): 62-65.
- Pardo, A., S. Feliu Jr., M.C. Merino, R. Arrabal and E. Matykina, 2010. Electrochemical estimation of the corrosion rate of magnesium/aluminium alloys. *Int. J. Corrosion*, 2010(2010): 8.
- Paul, S., 2012. Modeling to study the effect of environmental parameters on corrosion of mild steel in seawater using neural network. *ISRN Metall.*, 2012(2012): 6.
- Raja Dhas, J.E. and K. Somasundaram, 2013. Modeling and prediction of HAZ using finite element and neural network modeling. *Adv. Prod. Eng. Manage.*, 8(1): 13-24.
- Scully, J.R., 2000. Polarization resistance method for determination of instantaneous corrosion rates. *Corrosion*, 56(2): 199-218.
- Stansbury, E.E. and R.A. Buchanan, 2000. *Fundamentals of Electrochemical Corrosion*. ASM International, Materials Park, OH.
- Turgoose, S. and J.W. Palmer, 2005. Preferential weld corrosion of 1% Ni welds: Effects of solution conductivity and corrosion inhibitors. *Proceeding of CORROSION*, 2005. NACE International, Houston, TX, USA.